ACS APPLIED MATERIALS & INTERFACES

Research Article

www.acsami.org

Chemically Patterned Inverse Opal Created by a Selective Photolysis Modification Process

Tian Tian, Ning Gao, Chen Gu, Jian Li, Hui Wang, Yue Lan, Xianpeng Yin, and Guangtao Li*

Key Laboratory of Organic Optoelectronics & Molecular Engineering, Department of Chemistry, Tsinghua University, Beijing 100084, China

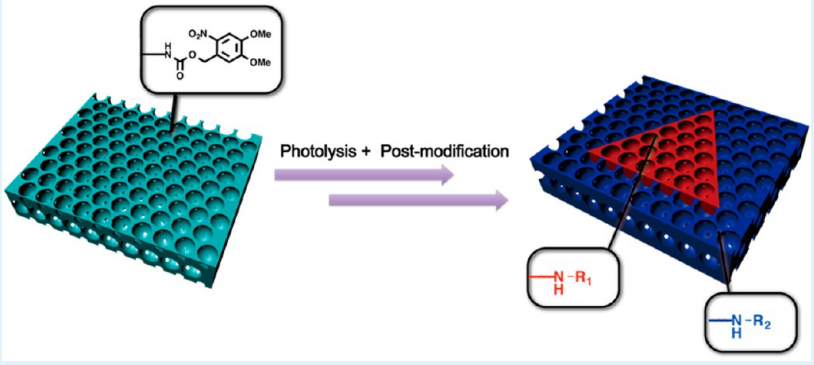

ABSTRACT: Anisotropic photonic crystal materials have long been pursued for their broad applications. A novel method for creating chemically patterned inverse opals is proposed here. The patterning technique is based on selective photolysis of a photolabile polymer together with postmodification on released amine groups. The patterning method allows regioselective modification within an inverse opal structure, taking advantage of selective chemical reaction. Moreover, combined with the unique signal self-reporting feature of the photonic crystal, the fabricated structure is capable of various applications, including gradient photonic bandgap and dynamic chemical patterns. The proposed method provides the ability to extend the structural and chemical complexity of the photonic crystal, as well as its potential applications.

KEYWORDS: *inverse opal, photolabile polymer, postmodification, patterning, photonic materials*

1. INTRODUCTION

The photonic crystal has emerged as a novel material, which has attracted intense attention from multiple disciplines. Its unique optical properties, signal self-reporting features, and highly periodic inner structure have led to numerous success in chemical sensing,[1−3] photonic circuits,[4] photonic displays,[5] macroporous electrodes,[6,7] etc. Despite its rapid development, applying photonic crystals for practical applications has one step beyond pure-color material, which is patterning. Patterning in a photonic crystal not only improves its use in applications such as anticounterfeiting materials and displaying but also introduces anisotropy or heterostructure, which highly extends the functionality of photonic crystals. Until now, much effort has been spent to achieve the goal of patterning a photonic crystal. The most studied methods involve patterning in opal-like and composite photonic crystal materials. Finely controlled swelling of substrate would partially alter the lattice spacing of a photonic crystal and therefore introduce a visible pattern. Fudouzi and Xia used a stamping method to introduce a silicon fluid-induced pattern into a poly(dimethylsiloxane) (PDMS)−polystyrene (PS) composite photonic crystal to achieve rewritable "photonic paper".[8] Variations of such a method include pH-induced photonic patterning[9] and a hygroscopic photonic pattern.[10,11] An inkjet printing approach is another way of directly fabricating a photonic pattern.[12,13] Electro- and magnetotuning of photonic structure has also been used in various works. Examples include an electro-driven photonic display using a ferrocene-containing polymer by Ozin et al.,[5] a dynamic photonic pattern tuned by a complex magnetic field,[14] a magneto-photonic pattern by stepwise phase fixation,[15] a magneto pattern by phase contrast,[16] etc. Lithography is another feasible yet more direct approach to fabricating a patterned photonic crystal. Using chemical[17,18] or physical lithography,[19,20] a three-dimensional pattern can be precisely introduced. The structural control of lithography also provides the possibility of more complex applications, for instance, photonic defects[21] or special wettability based on surface roughness.[22] The patterning in inverse opal structure is more challenging than an opal-like or composite photonic crystal. The integrity of inverse opal hinders the application of simple lithography. On the other hand, the intrinsic macroporous structure of a photonic crystal facilitates liquid diffusion within, which merely rules out the possibility of stamping or inkjet printing. Until now, several individual reports have dealt with

Received: July 24, 2015
Accepted: August 13, 2015
Published: August 13, 2015

DOI: 10.1021/acsami.5b06757
ACS Appl. Mater. Interfaces 2015, 7, 19516−19525

Scheme 1. Synthesis of the Compounds Used in This Work

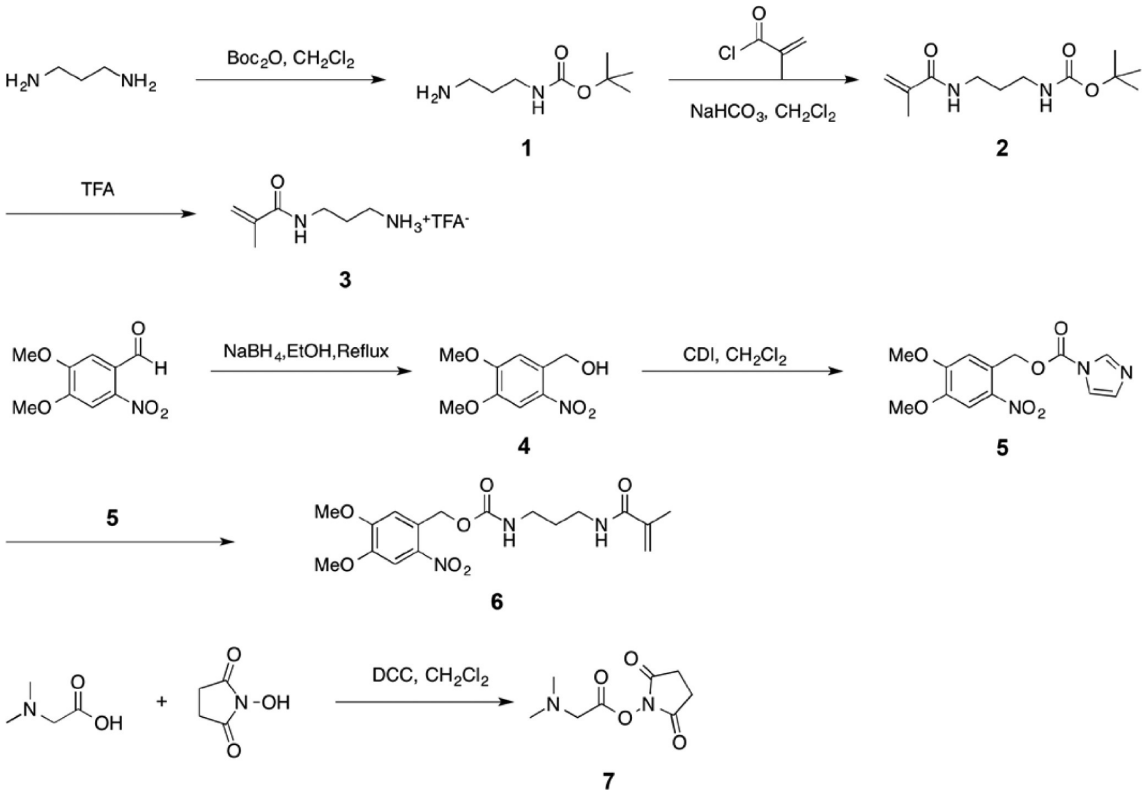

patterning in inverse opal. Wang et al. utilized stepwise polymerization to achieve inverse opal with a binary chemical composition.[23] Burgess et al. used reactive ion plasma to encode a complex chemical pattern in silica inverse opal.[24] However, such methods involved arduous procedures and lacked universality in creating a pattern in inverse opal, especially polymer-based inverse opal. Therefore, developing a novel and general strategy for patterning inverse opal is of significant research and practical interest.

In this work, a method for fabricating a chemical pattern in inverse opal is proposed, based on the combination of selective photolysis of a photolabile polymer and postmodification on released reactive groups. Such a method allowed control of the chemical component within inverse opal, which leads to its extendable functionality. With synergy of optical properties, a signal self-reporting feature, and a macroporous internal structure, several applications based on such chemically patterned inverse opal have been demonstrated, for instance, a gradient photonic bandgap and a dynamic chemical pattern. The proposed method not only creates a chemical pattern in inverse opal but also can extend its chemical component as well as functionality by postmodification. By combination with a photonic bandgap and other properties, such an approach holds great potential for the development of a photonic crystal with high complexity and functionality.

2. EXPERIMENTAL SECTION

2.1. Materials. All of the chemicals and solvents used in the experiments were of reagent quality, without further purification unless mentioned. Anhydrous ethanol, anhydrous methanol, ammonia, tetraethoxysilane (TEOS), sodium chloride (NaCl), sodium bicarbonate ($NaHCO_3$), and dichloromethane (DCM) were all purchased from SinoChem Co. Ltd. TEOS was distilled under vacuum (0.01 atm.) before use to remove impurities. DCM was dried by refluxing with calcium hydride (CaH_2) and distilled before use. Methyl methacrylate (MMA), ethylene glycol dimethacrylate (EGDMA), and azobis(isobutyronitrile) (AIBN) were bought from Acros Organics. Sodium borohydride ($NaBH_4$), 2-nitroveraldehyde, 1,3-diaminopropane, di-*tert*-butyl dicarbonate (Boc_2O), carbonyldiimidazole (CDI), *N*-hydroxysuccinimide (NHS), *N*,*N*′-dicyclohexylcarbodiimide (DCC), *N*,*N*-dimethylglycine, trifluoroacetic acid (TFA), methacryloyl chloride, and triethylamine (TEA) were obtained from Alfa Aesar. The flasks for Stöber silica sphere synthesis were treated by dichromate or piranha lotion before use. All glass slides were sheared out to be 50 mm × 20 mm, following piranha treatment, and rinsed with deionized water and anhydrous ethanol.

2.2. Characterization Methods. The ^1H nuclear magnetic resonance (NMR) spectra of substances were characterized by a JEOL ECA 300 NMR spectrometer. Reflectance spectra of photonic samples were measured by a USB2000 fiber spectrometer (Ocean Optics). The SEM images were taken by a LEO-1503 field emission scanning electron microscope. Contact angle tests were performed on an OCA 20 contact angle measurer (Dataphysics). Transmission UV−vis spectra were recorded with a Lambda 35 UV−vis spectrometer (PerkinElmer).

2.3. Synthesis of Compounds. The synthesis of compounds used in this work is depicted in Scheme 1.

2.3.1. Synthesis of Compound 1. 1,3-Diaminopropane (2.96 g, 40.0 mmol, 4 equiv) was dissolved in 100 mL of anhydrous DCM and stirred under an ice bath. A solution of 2.18 g (10.0 mmol, 1 equiv) of Boc_2O in 20 mL of DCM was slowly added dropwise into the flask. The adding procedure was completed within 30 min. With the addition of Boc_2O, a white precipitate began to form. After the completion of the addition, the reaction mixture was stirred at room temperature (rt) for an additional 16 h. The mixture was then filtered though a Buchner funnel to remove the white precipitate. The collected organic phase was washed three times with saturated saline, and the aqueous phase was then extracted with DCM once more. The combined organic phase was dried against anhydrous Na_2SO_4. The product (sticky transparent liquid) was obtained after vacuum evaporation (1.52 g, 87.0%).

DOI: 10.1021/acsami.5b06757
ACS Appl. Mater. Interfaces 2015, 7, 19516−19525

Compound **1** [*tert*-butyl (3-aminopropyl)carbamate]: ^{1}H NMR (300 MHz, $CDCl_3$) δ 1.31−1.62 (11H, m, $C(CH_3)_3$ and C-CH_2-C), 2.73 (2H, t, NH_2CH_2), 3.15 (2H, t, CONH-CH_2), 5.05 (2H, s, NH_2); ESI-MS 175.2 $[M + H]^+$.

2.3.2. Synthesis of Compound 2. Compound **1** (1.52 g, 8.70 mmol, 1 equiv)) was dissolved in 25 mL of DCM and mixed with 10 mL of a saturated $NaHCO_3$ solution. The mixture was vigorously stirred under an ice bath before the addition of 1.26 g (12.0 mmol, 1.4 equiv) of methacrylic chloride. The reaction mixture was kept at rt for an additional 30 min; 50 mL of DCM was added to the mixture, and the organic phase was separated and further washed twice with saturated saline. The organic phase was dried against Na_2SO_4 and evaporated under vacuum. The crude was refined by column chromatography (pure DCM) to obtain a white crystalline solid (1.18 g, 59.4%).

Compound **2** [*tert*-butyl (3-methacrylamidopropyl)carbamate]: ^{1}H NMR (300 MHz, $CDCl_3$) δ 1.35 (s, 9H, $C(CH_3)_3$), 1.64 (m, 2H, C-CH_2-C), 1.98 (s, 3H, CH_2-C═), 3.15 (t, 2H, BocNH-CH_2), 3.36 (t, 3H, acrylNH-CH_2), 5.39 (d, 1H, ═CH), 5.79 (d, 1H, ═CH); ESI-MS 243.6 $[M + H]^+$.

2.3.3. Synthesis of Compound 3. Compound **2** (1.94 g, 8.50 mmol) was disscolved in 10 mL of dry DCM and the mixture stirred under an argon atmosphere. Two milliliters of TFA was carefully added to the solution. Bubbles formed during the reaction process, and the pressure was gradually reduced in the flask to prevent explosion. The reaction mixture was kept at rt overnight. Excess TFA was removed by high vacuum under an ice bath (an overly high temperature will cause self-polymerization). The product was obtained after precipitation with ether (white solid to liquid, 0.884 g, 81.2%).

Compound **3** (3-methacrylamidopropan-1-aminium trifluoroacetate): ^{1}H NMR (300 MHz, DMSO-d_6) δ 1.64 (m, 2H, C-CH_2-C), 1.98 (s, 3H, CH_2-C═), 3.36 (t, 3H, acrylNH-CH_2), 5.39 (d, 1H, ═CH), 5.79 (d, 1H, ═CH), 7.66 (s, 3H, NH_3^+); ESI-MS 143.2 $[M + H]^+$.

2.3.4. Synthesis of Compound 4. 2-Nitroveraldehyde (4.22 g, 20.0 mmol, 2 equiv) was suspended in 150 mL of ethanol. After the mixture has been stirred, 0.378 g (10.0 mmol, 1 equiv) of $NaBH_4$ was slowly added to the suspension. The yellow solid gradually dissolved following the reaction process, and an orange solution was finally reached. The reaction was then allowed to continue at rt without light for an additional 5 h. The organic solvent was then evaporated. The crude product was refined by column chromatography [1:1 petroleum ether (PE)/ethyl ethatate (EA)] to yield a light orange solid (3.46 g, 81.3%).

Compound **4** [(4,5-dimethoxy-2-nitrophenyl)methanol]: ^{1}H NMR (300 MHz, $CDCl_3$) δ 2.66 (s, 1H, OH), 4.00 (d, 6H, -OMe), 4.98 (s, 2H, CH_2), 7.17 (s, 1H, Ph-H), 7.69 (s, 1H, Ph-H); ESI-MS 226.1 $[M + Na]^+$.

2.3.5. Synthesis of Compound 5. Compound **4** (1.82 g, 8.54 mmol, 1 equiv) was dissolved in 25 mL of anhydrous DCM; 1.38 g (8.54 mmol, 1 equiv) of CDI was added to the solution in three portions. The reaction mixture was then kept at rt for 20 h. The reaction mixture was then diluted to 100 mL and washed twice with saturated saline. The combined organic phase was then dried with Na_2SO_4 and evaporated. The product (light yellow solid) was obtained without further purification (2.45 g, 93.7%).

Compound **5** (4,5-dimethoxy-2-nitrobenzyl 1*H*-imidazole-1-carboxylate): ^{1}H NMR δ 4.00 (d, 6H, -OMe), 4.98 (s, 2H, CH_2), 7.03 (d, 1H, ═N-CH-CH), 7.17 (s, 1H, Ph-H), 7.40 (d, 1H, ═N-CH-CH), 7.69 (s, 1H, Ph-H), 8.13 (d, 1H, N═CH-N); ESI-MS 308.8 $[M + H]^+$

2.3.6. Synthesis of Compound 6. Compound **5** (1.12 g, 3.65 mmol, 1 equiv) and 1.5 mL of TEA were dissolved in 20 mL of andyhrous DCM and kept under an ice bath. While the mixture was being stirred, 1.14 g (4.75 mmol, 1.3 equiv) of compound **3** in 20 mL of DCM was slowly added to the solution for 1 h. After the completion of addition, the reaction mixture was kept in the dark and stirred for an additional 20 h. The solution was diluted to a total volume of 150 mL and washed with 1 M HCl and saturated saline. The organic phase was then dried against Na_2SO_4 and concentrated. Further purification was achieved by column chromatography (pure DCM) to obtain a white to light yellow powder (0.909 g, 65.4%).

Compound **6** [4,5-dimethoxy-2-nitrobenzyl (3-methacrylamidopropyl)carbamate]: ^{1}H NMR (300 MHz, $CDCl_3$) δ 1.98 (s, 3H, CH_2-C═), 3.36 (t, 3H, acrylNH-CH_2), 4.00 (d, 6H, -OMe), 4.98 (s, 2H, CH_2), 5.39 (d, 1H, ═CH), 5.79 (d, 1H, ═CH), 6.59 (s, 1H, CONH), 7.17 (s, 1H, Ph-H), 7.69 (s, 1H, Ph-H); ESI-MS 404.2 $[M + H]^+$.

2.3.7. Synthesis of Compound 7. *N*,*N*-Dimethylglycine (5.15 g, 50.0 mmol, 1 equiv) and 5.75 g (50.0 mmol, 1 equiv) of NHS were dissolved in 200 mL of anhydrous DCM; 11.05 g (55.0 mmol, 1.1equiv) of DCC was then carefully added to the mixture. The reaction mixture was then kept at rt for 20 h. The resulting white solid was filtered, and the solution was concentrated and further purified by column chromatography (1:2 PE/EA) to yield a white waxy solid (2.35 g, 23.2%).

Compound **7** (2,5-dioxocyclopentyl dimethylglycinate): ^{1}H NMR (300 MHz, $CDCl_3$) δ 2.42 (s, 6H, CH_3), 2.82 (s, 4H, CH_2CH_2), 3.52 (s, 2H, N-CH_2); ESI-MS 201.2 $[M + H]^+$.

2.3.8. Preparation of the SiO_2 Colloid Crystal Template. Monodisperse silica particles were synthesized by the modified Stöber method.[25] Ammonia (10−12 mL) and 100 mL of anhydrous ethanol were mixed and stirred in a 250 mL flask. Four milliliters of TEOS was then added to the solution quickly. The mixture was stirred at room temperature for 12 h. Monodisperse SiO_2 particles were obtained after centrifugation. The particles were further dispersed in anhydrous ethanol and centrifuged several times for purification. In this work, silica particles ∼250 nm in diameter were used for illustration.

The colloidal crystal template on a glass substrate was prepared by an extension of a monolayer silica arrangement preparation by surface tension.[26] (1) The silica particles were dried under vacuum and ground. A suspension of silica particles in *n*-butanol with a weight ratio of 0.1−0.4% was then prepared by sonication. The suspension was sonicated and centrifuged at 1000 rpm for 1 min to remove the large clusters. (2) Glass slides were cut, washed with piranha lotion, and placed in a clean glass Petri dish. The Petri dish was then treated with oxygen ion plasma for 1 min. (3) Deionized water was added to the Petri dish until the water level overwhelmed the glass slides. The gap between the glass slides and the water level was controlled to <2 mm. (4) The silica suspension prepared in step 1 was taken by syringe and slowly added to the water surface. With the addition of the suspension, a monolayer of silica was created on the water surface. The suspension was added until a closely packed monolayer was formed. After the Petri dish had been held for ∼5 min, excess water was then syringed to spread the silica monolayer on the top of glass slides. (5) The glass slides were dried in an oven at ∼50 °C until the residue solvent was removed. (6) Steps 2−5 were repeated, e.g., ion plasma treatment, monolayer generation, transfer, and drying, until a colloidal crystal with the desired number of layers was obtained. Considering both the optical quality of the photonic crystal and fabrication time, the number of layers was set to 10 in this work.

2.3.9. Preparation of Patterned Inverse Opal. The inverse opal-containing photolabile polymer was prepared by the following procedures. (1) Compound **6** (50.0 mg, 0.178 mmol), 30.2 mg (0.301 mmol) of MMA, and 6.5 mg (0.033 mmol) of EGDMA were dissolved in 20 μL of dimethyl sulfoxide (DMSO). The solution was heated to 60 °C to prevent precipitation of the functional monomer. AIBN [5% (w/w)] was then added to the solution and stirred. (2) A slide of the colloidal crystal template was used to adhere the silica-containing face with a poly(methyl methacrylate) (PMMA) slide of the same size. The monomer solution prepared in step 1 was added through the ridge of the sandwich structure, and the voids were infiltrated by capillary force. The mixture was carefully sealed by clamps and placed in an 80 °C oven to induce polymerization. The polymerization was continued for 24 h. (3) After being taken from the oven and cooled to rt, the sandwich structure was placed in a 2% hydrofluoric acid (HF) solution to etch the silica particles. (4) After completion of the etching process, the inverse opal-containing PMMA slide was separated from the glass slide. It was rinsed with a 1:1 H_2O/EtOH solvent to remove residual monomer and HF. The prepared inverse opal was then used for further photolysis and modification.

DOI: 10.1021/acsami.5b06757
ACS Appl. Mater. Interfaces 2015, 7, 19516−19525

Scheme 2. Principle of Photolysis of NVOC-Protected Amine Compounds

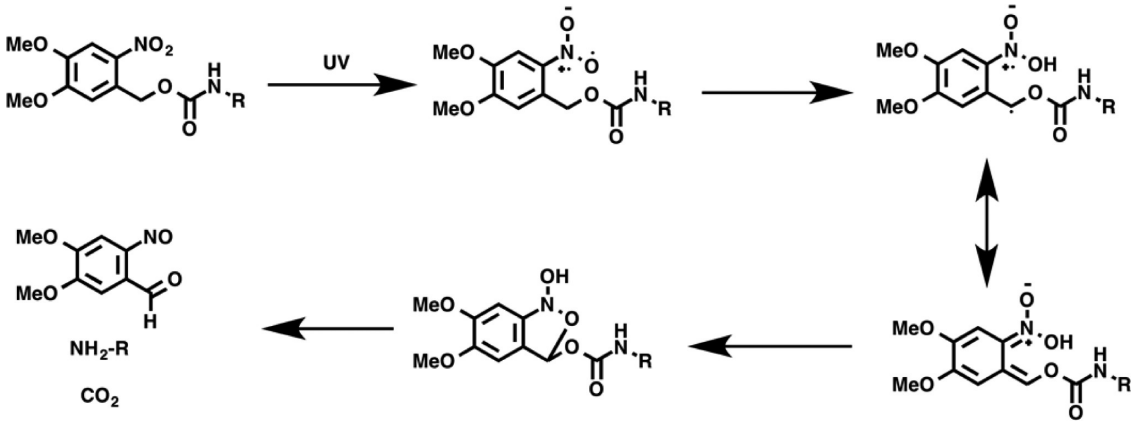

Scheme 3. Illustration of the Principle of the Chemical Patterning Process of Inverse Opal, Based on Selective Photolysis of an NVOC-Containing Polymer and Postmodification

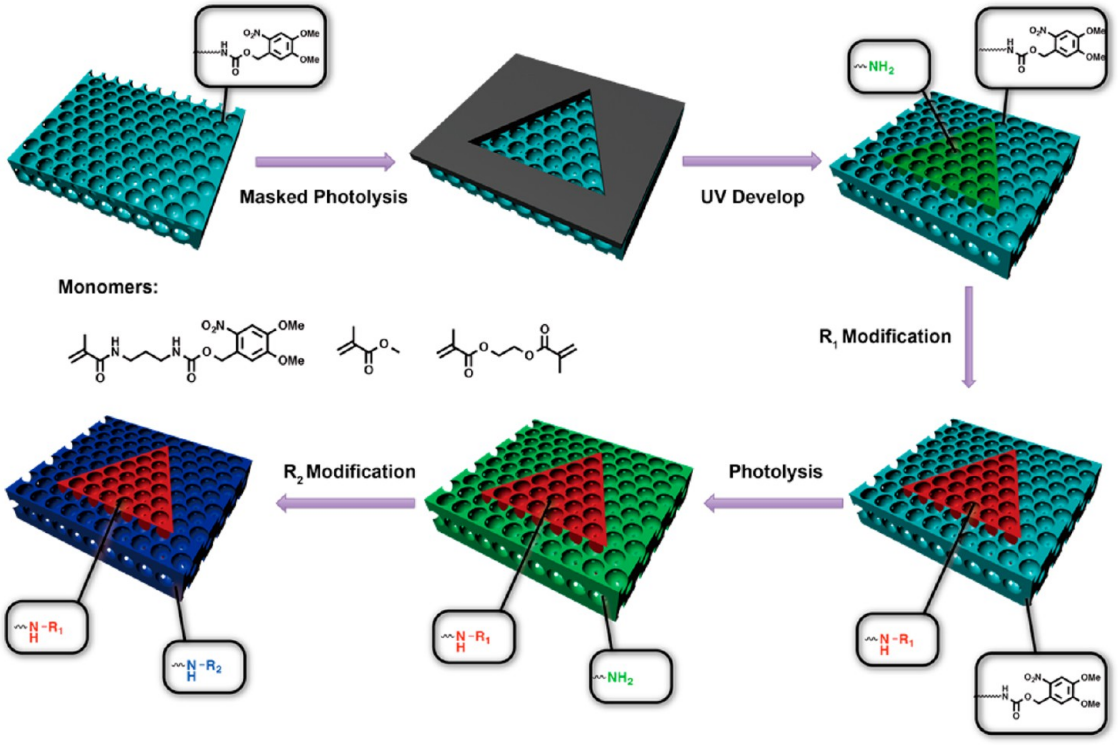

For the photolysis process, the inverse opal was adhered with the photomask and carefully wrapped by aluminum foil to protect the other parts from UV light. Photolysis was performed under a 200 W Hg UV lamp at a distance of 25 cm. The photolysis was conducted at a time interval of 10 s, and the process was typically completed within 3 min. After photolysis, the inverse opal was rinsed with a 1:1 H_2O/EtOH solvent to remove the residual chromophore.

For the modification process, the unprotected inverse opal was immersed in a solution of modification molecules [acetonitrile, dimethylformide (DMF), or DMSO as a solvent]. The reaction mixture was typically kept for 30 min. Excess reaction solution was absorbed by filter paper, and the polymer inverse opal was carefully washed with a 1:1 H_2O/EtOH solvent. For multiple-pattern modification, the inverse opal was further subjected to UV photolysis and modification of other functional groups.

3. RESULTS AND DISCUSSION

Herein, we propose a patterning strategy for inverse opal, which benefits from the combination of selective photolysis of a photolabile polymer and postmodification. The main principle behind such an approach is the photolabile group *N*-nitroveratryloxycarbonyl (NVOC). NVOC is a photosensitive protecting group commonly used in the protection of amino groups in amino acids.[27,28] The most promising property of the NVOC group is that it would undergo radical rearrangement under UV exposure and release the amine group (Scheme 2). Among all the photolabile group candidates, NVOC absorbs UV light at a relatively longer wavenumber (~360 nm),[29] which would be more suitable for processing in inverse opal, as shorter wavelength light (<280 nm) would cause degradation of the polymer. The other reason for choosing NVOC is that it would release one free amine group, which would facilitate

DOI: 10.1021/acsami.5b06757
ACS Appl. Mater. Interfaces 2015, 7, 19516−19525

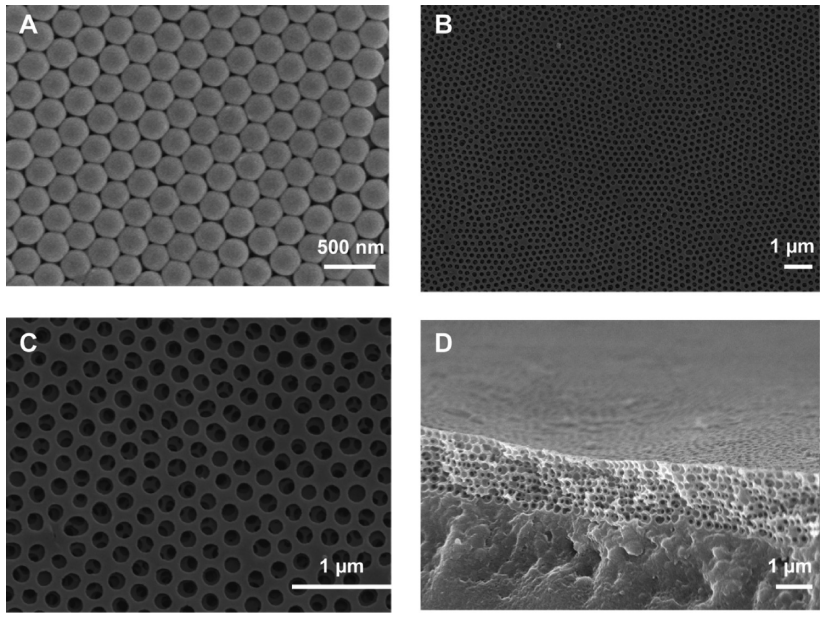

Figure 1. SEM characterization of the materials used in this work. (A) Silica colloidal template fabricated by the LbL method. (B) Large-area SEM photograph of the inverse opal. (C) SEM photograph of the NVOC-containing polymer inverse opal after UV exposure for 5 min. (D) Cross section of the inverse opal structure (indicating 10 layers of repeated structure).

further modification. On the other hand, other photolabile groups, which protect hydroxyl or carboxyl groups, would be harder to modify because of the relatively low reaction rate. The released amine groups after photolysis would be suitable for modification, if subjected to reactive compounds such as carboxyl chloride-activated ester. Such modification would be completed under mild conditions at a relatively acceptable rate, which allows postmodification of light-processed inverse opal.

On the basis of the principle described above, a strategy for fabricating inverse opal with a versatile chemical pattern is proposed, as illustrated in Scheme 3. Briefly, inverse opal made of the NVOC-containing polymer was fabricated by sequential template replication of a silica colloidal crystal and HF etching. The fabricated inverse opal was then subjected to masked UV exposure to selectively release free amine groups on a specific region, while the rest of the NVOC groups in other parts remained unaffected. The partially unprotected inverse opal was then reacted with the chosen reactive compound to induce modification. The specificity of chemical reaction plays an important role in the modification process: only the free amine groups would undergo condensation with the reactive compound, while the NVOC-protected ones remain inert to the reaction. The merit of such a selective reaction would overcome the diffusion problem caused by internal pores of inverse opal. In other words, the proposed method requires no regioselective manipulation of liquid, which is essential in other methods such as stamping and inkjet printing and makes the procedure more facile. Moreover, benefitting from the broad possibilities of amine functionalization, such a method is capable of creating multiple patterns with distinct chemical compositions as well as functionalities. Last but not least, the photonic basis of inverse opal further enriches the applications of such patterned material. Unlike patterning on a planar substrate, the photonic bandgap, signal self-reporting feature, and interconnected macroporous structure of inverse opal endow the structure with broad possibilities of application, as shown in this work.

To verify the feasibility of such a material and such a patterning method, several characterization approaches were performed. The inner structure of the colloidal template and its inverse opal replicates were studied by scanning electron microscopy (SEM). As demonstrated in Figure 1A, the colloidal crystal template made from layer-by-layer (LbL) deposition of monolayer silica particles showed a good hexagonal arrangement, which could be compared with those prepared by the evaporation-induced vertical deposition method,[3] proving the quality of the colloidal crystal made from such an approach. The SEM photographs in Figure 1C show a large-area hexagonal porous structure, with a diameter close to that of its template. It could be noted that the inverse opal prepared with the LbL template showed a large-area flat surface, and the macropores are evenly distributed at the surface, with merely no large line defects seen in the material prepared by the evaporation-induced method. The SEM images of both the template and the inverse opal strongly supported the good quality of the materials used in this work. An investigation of the effect of UV irradiation on the structure of NVOC-containing inverse opal was also conducted. The inverse opal was treated with UV for 5 min and rinsed to remove the cleaved residues. As seen in Figure 1C, minor destruction could be seen on the surface of the inverse opal, as a few junctions between pores are found to be discontinuous. This could be ascribed to the destruction of the polymer caused by UV light. If the preparation is taken into consideration, because NVOC is highly sensitive to UV light, the polymerization process could be conducted only using a thermo-radical initiator, such as AIBN. As the nitrophenyl moiety of NVOC would absorb the radical during the polymerization process, an excess of initiator was used versus that used in the normal polymerization process.[30] Both the long half-life of the thermo-radical initiator and its excessive amount caused a short polymer chain length and a low cross-link efficiency. As the unprotected polymer would turn more hydrophilic than its protected form, the polymer might be more fragile to solvent

DOI: 10.1021/acsami.5b06757
ACS Appl. Mater. Interfaces 2015, 7, 19516−19525

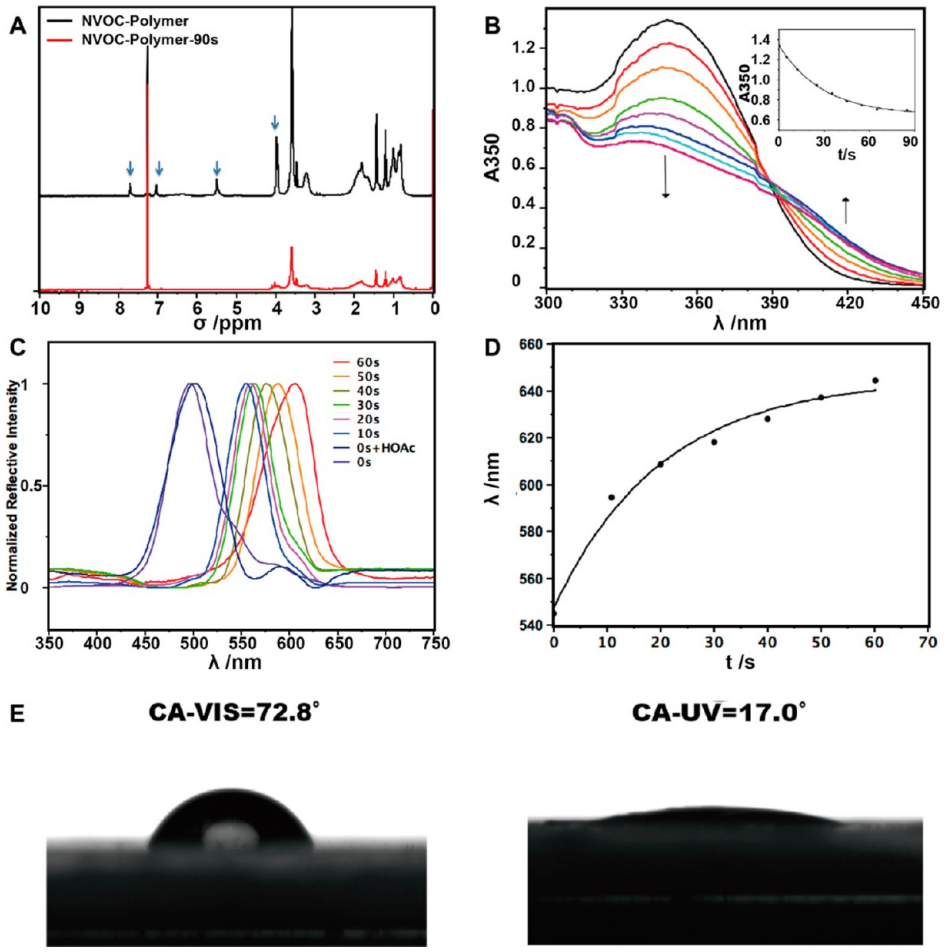

Figure 2. Characterizations of NVOC polymer inverse opal. (A) NMR spectra of the linear NVOC polymer before and after photolysis. (B) UV−vis spectra of the NVOC polymer. The inset shows the time-resolved curve of A_{350} change. (C) Reflection spectra (normalized) of NVOC inverse opal upon stepwise photolysis. (D) Time-resolved curve of the Bragg peak wavelength with exposure time. (E) Contact angles of the nonporous polymer surface before and after UV exposure.

after photolysis. Fortunately, only minor destruction could be observed, which proved that under the described condition, the polymer inverse opal still exhibited acceptable stability after photolysis. A cross-sectional SEM photograph of Figure 1D further showed that the structure of inverse opal was uniform within the whole material. The interconnected pores served as the basis by which the reaction solution could spread within the inverse opal, and the chance that reaction occurred was equal throughout the bulk polymer.

The reactivity and efficiency of the NVOC-containing polymer are other key factors that affect such a patterning method. Infrared (IR) spectra would be the most direct evidence of reaction. However, as the vibration of the nitro group highly overlaps with that of the carboxyl group (e.g., the amide and carbamate group in the monomers used here), it was hard to find the change before and after photolysis. Therefore, we utilized the NMR spectra instead to reveal the chemical composition change. For illustration, a linear polymer that consisted of an NVOC monomer (compound **6**) and MMA was prepared using the same monomer ratio as the cross-link polymer, while EGDMA was absent. As demonstrated in Figure 2A, the signals at 7.67 and 6.98 ppm corresponded to the phenyl hydrogens in the NVOC group, while the peaks at 5.41 and 4.02 ppm were those of methylene and methoxyl hydrogens, respectively. Together with the methyl H at 3.53 ppm of PMMA, the content of NVOC groups in the prepared polymer was calculated to be 17.6%, almost half of the monomer ratio in the precursor solution. This also supported the findings that NVOC monomers are difficult to polymerize.[31] As the ratio in the precursor solution remained the same, the ratio of NVOC groups in the linear polymer could also reflect the ratio in the cross-link polymer. After UV exposure for 60 s, the $CDCl_3$ solution of the polymer turned dark brown, which resulted from the released chromophore after unprotection (Scheme 1). The complete diminishing of the NVOC peaks at 7.67, 6.98, 5.41, and 4.02 ppm strongly supported the completion of the photolysis process.

As the NVOC group underwent a structural change during photolysis, its UV−vis absorption spectra could also be used to estimate the degree of reaction. We used a nonporous film for such a measurement. As seen in Figure 2B, the absorption peaks at 350 nm (from the conjugated NVOC group) ceased to it baseline (which appeared as a sloped line due to scattering of the substrate), while the intensity of the peak at 420 nm (the release chromophore) increased slightly. The transformed $A_{350}-t$ curve in the inset proved that the photolysis process was completed within 90 s. The slightly elongated photolysis time was apparently due to the cross-link in the polymer network, which hinders the movement of a single moiety. Via combination of the evidence of NMR and UV−vis character-

DOI: 10.1021/acsami.5b06757
ACS Appl. Mater. Interfaces 2015, 7, 19516−19525

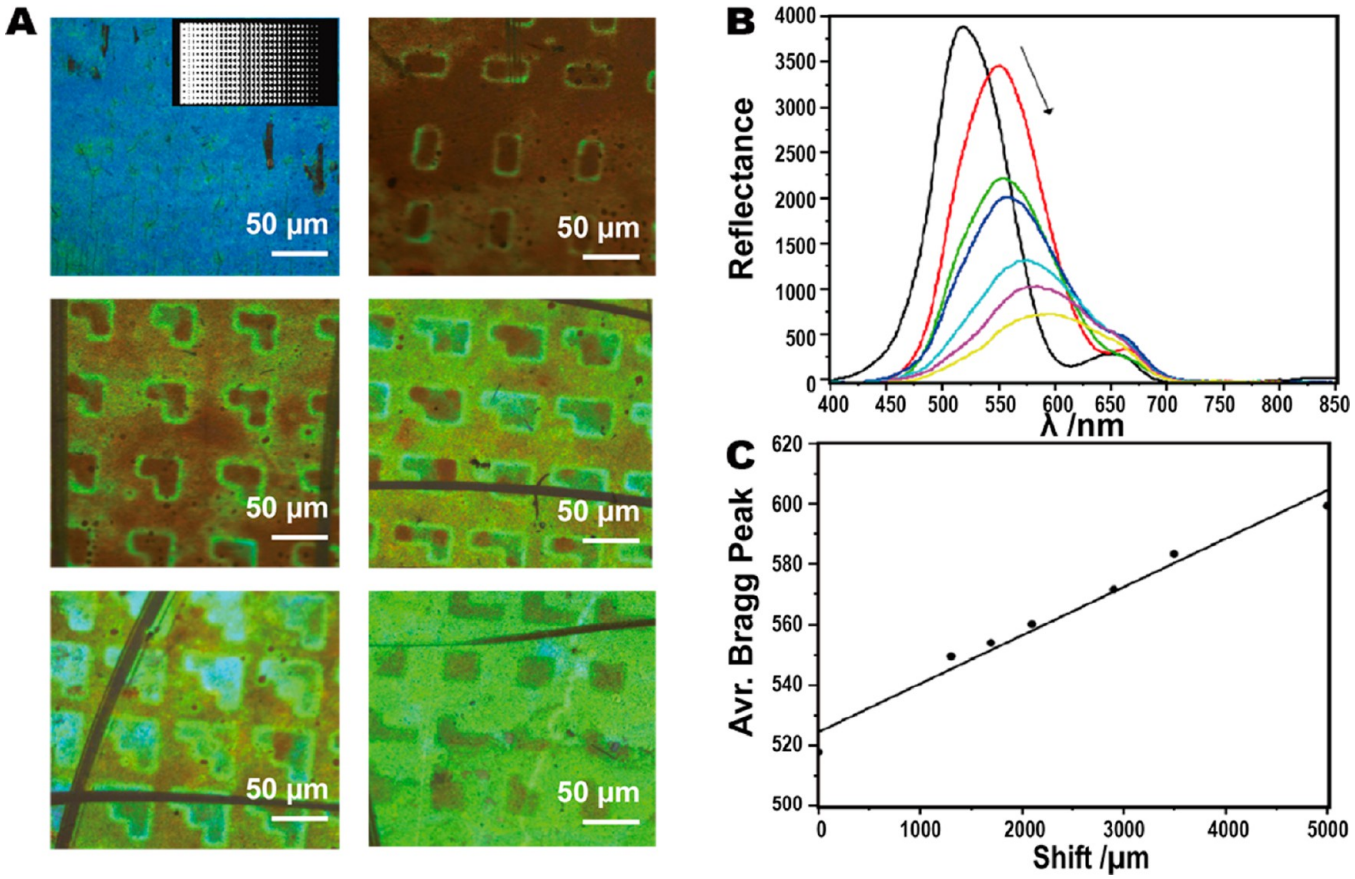

Figure 3. Inverse opal with a hydrophilicity gradient pattern. (A) Microscopy photographs of inverse opal before (first) and after (rest) the photoprocess. The inset shows a predesigned photomask with a gradient generated by binary blocks. The patterns correspond to left to right regions in the photomask. (B) Reflection spectra of the gradient pattern inverse opal. (C) Plot of the spectral central wavelength with its position.

ization, the photolysis of the NVOC polymer was rapid and efficient. Such properties allow the facile operation of patterned inverse opals.

A further step was taken to investigate the combination of photonic structure with the NVOC-containing polymer. The inverse opal was treated with UV exposure at time intervals of 10 s, and their reflection spectra were recorded. It could be seen in Figure 2C that the reflection peak (i.e., the photonic bandgap) underwent a gradual red shift upon UV photolysis. The central position of the photonic bandgap of photonic crystal could be expressed by the Bragg diffraction equation (eq 1):

$$\lambda = 2d\sqrt{\sum_{i}^{m} n_i^2 f_i - \sin^2\theta} \quad (1)$$

whereas the wavelength of central peak λ is governed by lattice spacing d, refractive indices n, and their space portion. During photolysis, the UV-cleaved NVOC polymer released free amine groups, which increased the hydrophilicity of the polymer. As a result, the polymer would exhibit both swelling behavior and water permeation. Both would cause the red shift of the photonic bandgap. The time-resolved peak shift curve in Figure 2D also proved this. Moreover, the sigmoid-shaped curve revealed that the photolysis would have saturation upon stepwise UV exposure. More evidence of the hydrophilicity change could be derived from the contact angle test. As seen in Figure 2E, the contact angle of the nonporous film decreased sharply from 72.8° before irradiation to 17.0° after photolysis. Such a large change in contact angle could only be the result of released amine after photolysis. In conclusion, characterization methods proved that the chemical composition changed after photolysis. With a combination of a selective photoprocess and photonic structure, it is feasible to fabricate chemically patterned inverse opal using the proposed method.

Taking advantage of the rapid and effective photolysis of the NVOC polymer, we were able to construct patterned inverse opal using a designed photomask. As a demonstration, we tried to fabricate a hydrophilicity gradient pattern on a three-dimensional photonic crystal. As the sharp hydrophilicity change before and after photolysis, the hydrophilicity gradient could be prepared by integrating patterns with different degrees of photolysis. Here we used a predesigned binary gradient photomask to achieve such a goal. Because that grayscale phot mask was not available from our manufacturer, a binary photomask was used instead. As seen in the inset of Figure 3A, the photomask consisted of 20 μm square binary blocks. The gradient was simulated by randomly sampling blocks to achieve an approximate linear distribution, which was generated by a homemade program. Via application of such a photomask, exposure of the inverse opal to UV light, and development of the pattern with an acidic aqueous solution, the corresponding gradient pattern could be observed (Figure 3A, from top to bottom). For each area in the inverse opal, the reflection spectra would be the average of the exposed and unexposed regions. Unexpected brighter rims around the patterned areas could be observed in Figure 3A. Considering the system we have used, it might result from the inhomogeneous chemical

DOI: 10.1021/acsami.5b06757
ACS Appl. Mater. Interfaces 2015, 7, 19516−19525

nature near the pattern region, which resulted from diffraction of the photomask edge. Using a highly flat substrate may help to improve the quality of the patterns. The spectra in Figure 3B reveal the regio-dependent spectral shift, with the light spot measurement area being 500 μm in diameter (~10 repeating patterned units). The spectral behavior corresponded well to its hydrophilic gradient nature. More in-depth study of the dependence of the reflection spectra with the displacement of the measured area showed that the average spectra linearly correlated with its position, which was of high consistency with the designed gradient. Such prototype gradient-patterned inverse opal showed the power of controlling the regio-specific chemical composition and optical properties using the proposed photolysis method.

Moreover, inverse opal material with a gradient pattern provides various possibilities in fields such as chemical sensing,[32] photonic crystal-based spectrometry,[33] directional liquid transfer within inverse opal,[34] etc.

In addition to the pattern fabricated by a single photoprocess, we further studied the possibility that multiple chemical patterns can be prepared via a photolysis modification process. Herein, for the purpose of illustration, we implemented inverse opal with two chemically different patterns by the aforementioned method. One pattern was treated with propyl isocyanate so that the opal was chemically inert, while the other pattern was modified by the ternary amine (compound 7). The ternary amine group exhibits good pH-dependent switching behavior. Because of its mild alkaline property, the protonation process of ternary amine could be reversibly controlled by CO_2/N_2 cycles (Scheme 4).[35]

Scheme 4. Principle of Reversible Protonation of Ternary Amine under a CO_2/N_2 Cycle

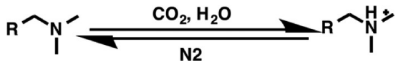

Therefore, on the basis of the distinct chemical component of separated patterns, it is highly desirable that a dynamically controllable photonic pattern could be realized using such a method. As seen in Figure 4A, the fabricated patterned inverse opal exhibited a distinct appearance in transmission and reflection mode. In transmission mode, the photonic crystal had a transparent appearance, with its color shown as the reciprocal of the reflection light. While in the reflection mode, light was strongly reflected, showing the structural color as well as its pattern, and hiding the letters on the background. The "THU"-shaped pattern (THU stands for the authors' institute) consisted of the inert propyl isocyanate-modified region, while the background was reacted with compound 7. The initial pattern was shown by the contrast of the reflective indices of these two parts. Moreover, the functionality difference allowed dynamic patterning of such material. As shown in Figure 4A, the protonated inverse opal exhibited a clear pattern and boundary.

The Bragg refraction peaks of the two regions were at 122 nm (Figure 4B). However, when CO_2 was bubbled in water, the outer pattern quickly red-shifted, making the two patterns less distinguishable, which could be seen in both whole-scale and microscopy photographs. The spectra revealed that the difference between these two patterns was held to 35 nm, which was mainly contributed by the red shift of the ternary pattern, while the structural color of the inert pattern remained almost unchanged. Such a gas-responsive pattern could be utilized for fabrication of commercial labeling as well as anticounterfeiting materials. In addition, we also studied the responsive properties of such patterned material. As demonstrated in panels A and B of Figure 5, the Bragg peak of the responsive pattern showed high fidelity during the five cycles of CO_2/N_2 treatment. In addition, it was also exhibited a rapid responsiveness. As shown in Figure 5C, the responsive pattern had a fast response toward CO_2. Saturation analysis in Figure 5D also supported such a conclusion. Although the final equilibrium of protonation would not be reached for more than

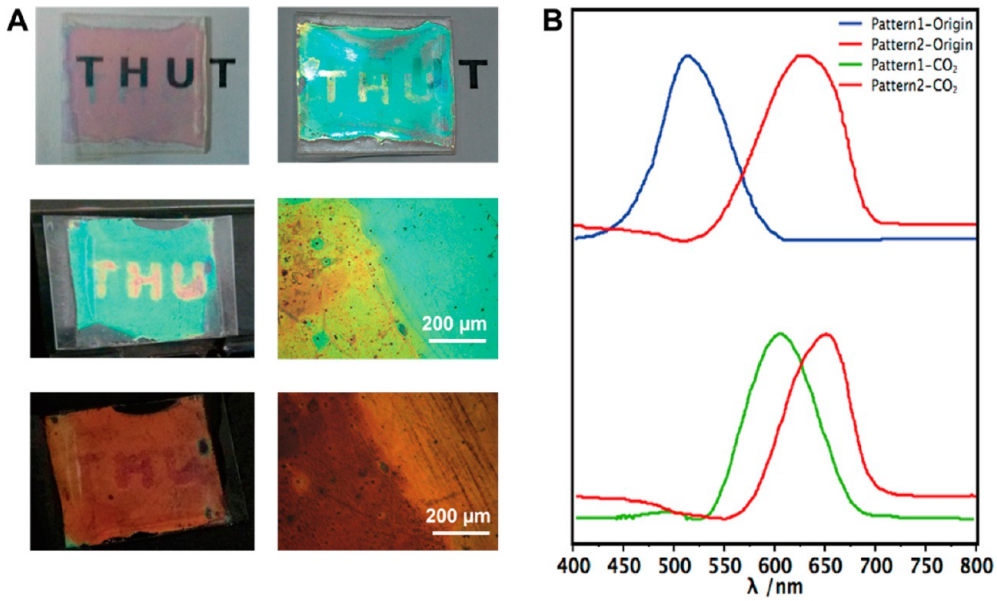

Figure 4. Dynamic chemical pattern in inverse opal. (A) Real sample of fabricated patterned inverse opal in transmission and reflection mode (top row). Patterned inverse opal under neutral conditions (middle row). Patterned inverse opal under protonated conditions (bottom row). (B) Reflection spectra of two patterns under neutral and protonated conditions.

DOI: 10.1021/acsami.5b06757
ACS Appl. Mater. Interfaces 2015, 7, 19516−19525

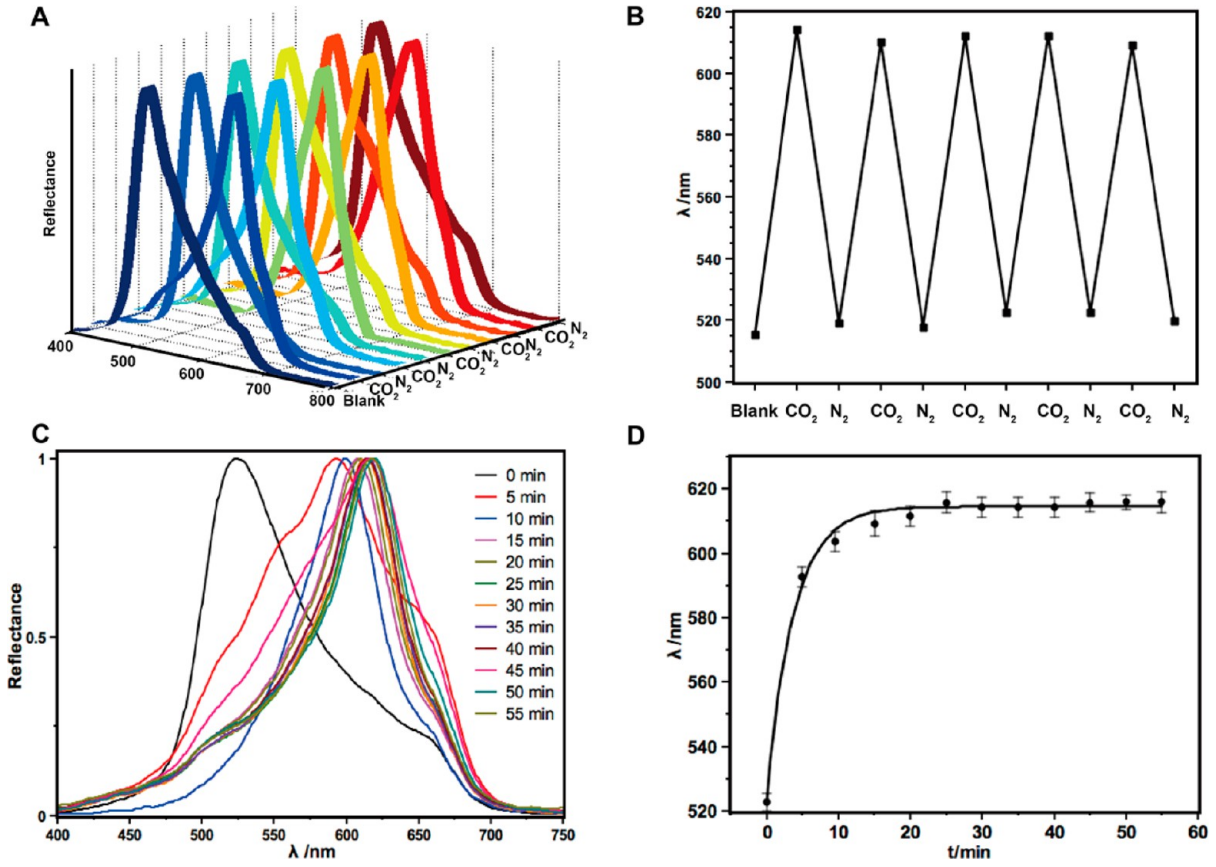

Figure 5. Responsiveness of pattern inverse opal. (A) Reflection spectra under CO_2/N_2 cycles. (B) Cycle behavior of the peak wavelength that corresponds to panel A. (C) Reflection spectra of the response to CO_2. (D) Saturation curve of the response to CO_2, corresponding to panel C.

20 min, the reaction with CO_2 in the first 5 min contributed to >75% of the Bragg peak shift, which could be used in rapid sensing applications. Such dynamic patterned inverse opal exhibited excellent reversibility. In conclusion, we have utilized the photolysis modification method to achieve dynamic patterning within inverse opal material. Such dynamically patterned photonic crystal material based on reversible CO_2/N_2 responsiveness has potential application in CO_2 sensing and anticounterfeiting material, which provides a visual approach for CO_2 indication. It should be noted that because of the vast extendability of such a platform, chemically patterned photonic crystals are not limited to the applications described above. It is foreseeable that such an approach would be a great candidate for developing a photonic crystal with a more complex chemical composition as well as a more complex functionality.

4. CONCLUSIONS

On the basis of photolabile NVOC-containing polymer, a patterning method for inverse opal was proposed by the combination of photolysis and postmodification. The rapid photolysis of the NVOC polymer together with the selectivity of amine modification ensures a regio-specific chemical pattern within inverse opal using a mild and facile approach. A photonic crystal with complex functionality could be realized by integrating the unique bandgap property, signal self-reporting feature, and macroporous structure of inverse opal with a spatially dependent chemical composition and responsiveness. Several applications were proposed on the basis of such a structure–function relationship, including a gradient hydrophilicity pattern and a dynamic chemical pattern. Because of the facile photolysis and versatile modification possibilities, the proposed method universally serves for the fabrication of photonic crystal materials with more complex structure and functionality. Via the introduction of structural and chemical anisotropy into inverse opal, such a method may find broad potential applications in fields like optical tuning, photonic sensing, anticounterfeiting materials, etc.

AUTHOR INFORMATION

Corresponding Author

*Key Laboratory of Organic Optoelectronics & Molecular Engineering, Department of Chemistry, Tsinghua University, Beijing 100084, China. E-mail: lgt@mail.tsinghua.edu.cn.

Funding

Supported by NSF China (20141300592, 21121004, and 20141311257), MOST Programs (2011CB808403 and 2013CB834502), and the Deutsche Forschungsgemeinschaft DFG (TRR61).

Notes

The authors declare no competing financial interest.

REFERENCES

(1) Asher, S. A.; Sharma, A. C.; Goponenko, A. V.; Ward, M. M. Photonic Crystal Aqueous Metal Cation Sensing Materials. *Anal. Chem.* **2003**, *75*, 1676–1683.

(2) Li, X.; Peng, L.; Cui, J.; Li, W.; Lin, C.; Xu, D.; Tian, T.; Zhang, G.; Zhang, D.; Li, G. Reactive Photonic Film for Label-Free and Selective Sensing of Cyanide. *Small* **2012**, *8*, 612–618.

(3) Tian, T.; Li, X.; Cui, J.; Li, J.; Lan, Y.; Wang, C.; Zhang, M.; Wang, H.; Li, G. Highly Sensitive Assay for Acetylcholinesterase

DOI: 10.1021/acsami.5b06757
ACS Appl. Mater. Interfaces 2015, 7, 19516–19525

Activity and Inhibition Based on a Specifically Reactive Photonic Nanostructure. *ACS Appl. Mater. Interfaces* **2014**, *6*, 15456−15465.
(4) Andress, W. F.; Yoon, H.; Yeung, K. Y. M.; Qin, L.; West, K.; Pfeiffer, L.; Ham, D. Ultra-Subwavelength Two-Dimensional Plasmonic Circuits. *Nano Lett.* **2012**, *12*, 2272−2277.
(5) Arsenault, A. C.; Puzzo, D. P.; Manners, I.; Ozin, G. A. Photonic-Crystal Full-Colour Displays. *Nat. Photonics* **2007**, *1*, 468−472.
(6) Chae, W.-S.; Van Gough, D.; Ham, S.-K.; Robinson, D. B.; Braun, P. V. Effect of Ordered Intermediate Porosity on Ion Transport in Hierarchically Nanoporous Electrodes. *ACS Appl. Mater. Interfaces* **2012**, *4*, 3973−3979.
(7) Arsenault, E.; Soheilnia, N.; Ozin, G. A. Periodic Macroporous Nanocrystalline Antimony-Doped Tin Oxide Electrode. *ACS Nano* **2011**, *5*, 2984−2988.
(8) Fudouzi, H.; Xia, Y. Colloidal Crystals with Tunable Colors and Their Use as Photonic Papers. *Langmuir* **2003**, *19*, 9653−9660.
(9) Liu, J.; Li, G.; Wu, Z.; An, Q.; Qiu, Y. A Poly(4-Vinylpyridine)-Based Inverse Opal. *ChemPhysChem* **2007**, *8*, 1298−1302.
(10) Ge, J.; Goebl, J.; He, L.; Lu, Z.; Yin, Y. Rewritable Photonic Paper with Hygroscopic Salt Solution as Ink. *Adv. Mater.* **2009**, *21*, 4259−4264.
(11) Xuan, R.; Ge, J. Invisible Photonic Prints Shown by Water. *J. Mater. Chem.* **2012**, *22*, 367−372.
(12) Cui, L.; Li, Y.; Wang, J.; Tian, E.; Zhang, X.; Zhang, Y.; Song, Y.; Jiang, L. Fabrication of Large-Area Patterned Photonic Crystals by Ink-Jet Printing. *J. Mater. Chem.* **2009**, *19*, 5499−5502.
(13) Wang, L.; Wang, J.; Huang, Y.; Liu, M.; Kuang, M.; Li, Y.; Jiang, L.; Song, Y. Inkjet Printed Colloidal Photonic Crystal Microdot with Fast Response Induced by Hydrophobic Transition of poly(N-Isopropyl Acrylamide). *J. Mater. Chem.* **2012**, *22*, 21405−21411.
(14) He, L.; Hu, Y.; Han, X.; Lu, Y.; Lu, Z.; Yin, Y. Assembly and Photonic Properties of Superparamagnetic Colloids in Complex Magnetic Fields. *Langmuir* **2011**, *27*, 13444−13450.
(15) Kim, H.; Ge, J.; Kim, J.; Choi, S.; Lee, H.; Lee, H.; Park, W.; Yin, Y.; Kwon, S. Structural Colour Printing Using a Magnetically Tunable and Lithographically Fixable Photonic Crystal. *Nat. Photonics* **2009**, *3*, 534−540.
(16) Xuan, R.; Ge, J. Photonic Printing through the Orientational Tuning of Photonic Structures and Its Application to Anticounterfeiting Labels. *Langmuir* **2011**, *27*, 5694−5699.
(17) Lange, B.; Zentel, R.; Ober, C.; Marder, S. Photoprocessable Polymer Opals. *Chem. Mater.* **2004**, *16*, 5286−5292.
(18) Lee, S.-K.; Yi, G.-R.; Moon, J. H.; Yang, S.-M.; Pine, D. J. Pixellated Photonic Crystal Films by Selective Photopolymerization. *Adv. Mater.* **2006**, *18*, 2111−2116.
(19) Ding, T.; Luo, L.; Wang, H.; Chen, L.; Liang, K.; Clays, K.; Song, K.; Yang, G.; Tung, C.-H. Patterning and Pixelation of Colloidal Photonic Crystals for Addressable Integrated Photonics. *J. Mater. Chem.* **2011**, *21*, 11330−11334.
(20) Lee, S. Y.; Kim, S.-H.; Hwang, H.; Sim, J. Y.; Yang, S.-M. Controlled Pixelation of Inverse Opaline Structures Towards Reflection-Mode Displays. *Adv. Mater.* **2014**, *26*, 2391−2397.
(21) Yan, Q.; Zhou, Z.; Zhao, X. S.; Chua, S. J. Line Defects Embedded in Three-Dimensional Photonic Crystals. *Adv. Mater.* **2005**, *17*, 1917−1920.
(22) Kang, H.; Lee, J.-S.; Chang, W. S.; Kim, S.-H. Liquid-Impermeable Inverse Opals with Invariant Photonic Bandgap. *Adv. Mater.* **2015**, *27*, 1282−1287.
(23) Wang, J.; Han, Y. Tunable Multicolor Pattern and Stop-Band Shift Based on Inverse Opal Hydrogel Heterostructure. *J. Colloid Interface Sci.* **2011**, *357*, 139−146.
(24) Burgess, I. B.; Mishchenko, L.; Hatton, B. D.; Kolle, M.; Loncar, M.; Aizenberg, J. Encoding Complex Wettability Patterns in Chemically Functionalized 3D Photonic Crystals. *J. Am. Chem. Soc.* **2011**, *133*, 12430−12432.
(25) Stöber, W.; Fink, A.; Bohn, E. Controlled Growth of Monodisperse Silica Spheres in the Micron Size Range. *J. Colloid Interface Sci.* **1968**, *26*, 62−69.
(26) Moon, G. D.; Lee, T. I.; Kim, B.; Chae, G.; Kim, J.; Kim, S.; Myoung, J.-M.; Jeong, U. Assembled Monolayers of Hydrophilic Particles on Water Surfaces. *ACS Nano* **2011**, *5*, 8600−8612.
(27) Barltrop, J. A.; Schofield, P. 883. Organic Photochemistry. Part II. Some Photosensitive Protecting Groups. *J. Chem. Soc.* **1965**, 4758−4765.
(28) Cameron, J. F.; Frechet, J. M. J. Photogeneration of Organic Bases from O-Nitrobenzyl-Derived Carbamates. *J. Am. Chem. Soc.* **1991**, *113*, 4303−4313.
(29) Zhao, H.; Sterner, E. S.; Coughlin, E. B.; Theato, P. O-Nitrobenzyl Alcohol Derivatives: Opportunities in Polymer and Materials Science. *Macromolecules* **2012**, *45*, 1723−1736.
(30) Schumers, J.-M.; Fustin, C.-A.; Can, A.; Hoogenboom, R.; Schubert, U. S.; Gohy, J.-F. Are O-Nitrobenzyl (meth)acrylate Monomers Polymerizable by Controlled-Radical Polymerization? *J. Polym. Sci., Part A: Polym. Chem.* **2009**, *47*, 6504−6513.
(31) Cui, J.; Nguyen, T.-H.; Ceolín, M.; Berger, R.; Azzaroni, O.; del Campo, A. Phototunable Response in Caged Polymer Brushes. *Macromolecules* **2012**, *45*, 3213−3220.
(32) Krabbenborg, S. O.; Huskens, J. Electrochemically Generated Gradients. *Angew. Chem., Int. Ed.* **2014**, *53*, 9152−9167.
(33) Ding, H.; Liu, C.; Gu, H.; Zhao, Y.; Wang, B.; Gu, Z. Responsive Colloidal Crystal for Spectrometer Grating. *ACS Photonics* **2014**, *1*, 121−126.
(34) Lee, J.-T.; George, M. C.; Moore, J. S.; Braun, P. V. Multiphoton Writing of Three-Dimensional Fluidic Channels within a Porous Matrix. *J. Am. Chem. Soc.* **2009**, *131*, 11294−11295.
(35) Han, D.; Tong, X.; Boissière, O.; Zhao, Y. General Strategy for Making CO2-Switchable Polymers. *ACS Macro Lett.* **2012**, *1*, 57−61.

DOI: 10.1021/acsami.5b06757
ACS Appl. Mater. Interfaces 2015, 7, 19516−19525